

CONF-9706113--8

SAN097-1949C  
SAND--97-1949C

## D-DOT AND B-DOT MONITORS FOR Z-VACUUM-SECTION POWER-FLOW MEASUREMENTS

W. A. Stygar, R. B. Spielman, H. C. Ives, W. B. S. Moore, J. F. Seamen, and A. W. Sharpe  
Sandia National Laboratories  
Albuquerque, New Mexico, USA

T. C. Wagoner, T. L. Gilliland, R. S. Broyles, J. A. Mills, T. A. Dinwoodie, and J. S. Slopek  
Ktech Corporation  
Albuquerque, New Mexico, USA

K. W. Struve  
Mission Research Corporation  
Albuquerque, New Mexico, USA

P. G. Reynolds  
Team Specialty Products  
Albuquerque, New Mexico, USA

### ABSTRACT

New differential D-dot and B-dot monitors were developed for the Z vacuum section. The D-dots measure voltage at the insulator stack. The B-dots measure current at the stack and in the outer magnetically-insulated transmission lines. Each monitor has two outputs that allow common-mode noise to be cancelled to first order. The differential D-dot has one signal and one noise channel; the differential B-dot has two signal channels with opposite polarities. Each of the two B-dot sensors in the differential B-dot monitor has four 3-mm-diameter loops and is encased in copper to reduce flux penetration. For both types of probes, two 2.2-mm-diameter coaxial-cables connect the outputs to a Prodyn balun for common-mode-noise rejection. The cables provide reasonable bandwidth and generate acceptable levels of Compton drive in Z's bremsstrahlung field. A new cavity B-dot is being developed to measure the total Z current 4.3 cm from the axis of the z-pinch load. All of the sensors are calibrated with 2-4% accuracy. The monitor signals are reduced with Barth or Weinschel attenuators, recorded on Tektronix 0.5-ns/sample digitizing oscilloscopes, and software cable compensated and integrated.

### I. INTRODUCTION

The 36-module Z accelerator<sup>1</sup> - designed to drive z-pinch loads at currents up to 20 MA - is contained in a 33-m-diameter tank with oil, water,<sup>2,3</sup> and vacuum<sup>4-10</sup> sections. The peak total forward-going power in the 36 water-section bi-plate transmission lines is approximately 63 TW.<sup>2,11</sup> Nine transmission lines deliver power to each of the four vacuum-section levels (referred to as levels A (the uppermost), B, C, and D).<sup>4-6</sup>

To monitor the vacuum-section performance, new differential D-dot and B-dot probes were developed. Six of the D-dots and three B-dots are fielded in each of the four Z-insulator-stack modules; in addition, six B-dots measure the current in each of the four outer magnetically-insulated transmission lines (MITLs).<sup>4,6</sup> A new cavity B-dot design is being tested to measure the total Z current 4.3 cm from the axis of the z-pinch load.

The differential D-dot and B-dot probes are described in Sec.'s II and III, respectively. The status of the cavity B-dot development is reported in Sec. IV. Results of Z-vacuum-section power-flow measurements are presented in Sec. V.

### II. DIFFERENTIAL D-DOT DESIGN AND CALIBRATION

The differential D-dots are mounted in the insulator-stack anode rings as shown in Figure 1. Each of the 24 monitors is located at the same radius, between an anode triple junction and an O-ring groove. Two-dimensional electrostatic ELECTRO<sup>12</sup> simulations show that the perturbation of the electric field at the vacuum-insulator interface by the monitors is negligible.

DISTRIBUTION OF THIS DOCUMENT IS UNLIMITED

ng MASTER

# **DISCLAIMER**

**Portions of this document may be illegible in electronic image products. Images are produced from the best available original document.**

### **DISCLAIMER**

This report was prepared as an account of work sponsored by an agency of the United States Government. Neither the United States Government nor any agency thereof, nor any of their employees, make any warranty, express or implied, or assumes any legal liability or responsibility for the accuracy, completeness, or usefulness of any information, apparatus, product, or process disclosed, or represents that its use would not infringe privately owned rights. Reference herein to any specific commercial product, process, or service by trade name, trademark, manufacturer, or otherwise does not necessarily constitute or imply its endorsement, recommendation, or favoring by the United States Government or any agency thereof. The views and opinions of authors expressed herein do not necessarily state or reflect those of the United States Government or any agency thereof.

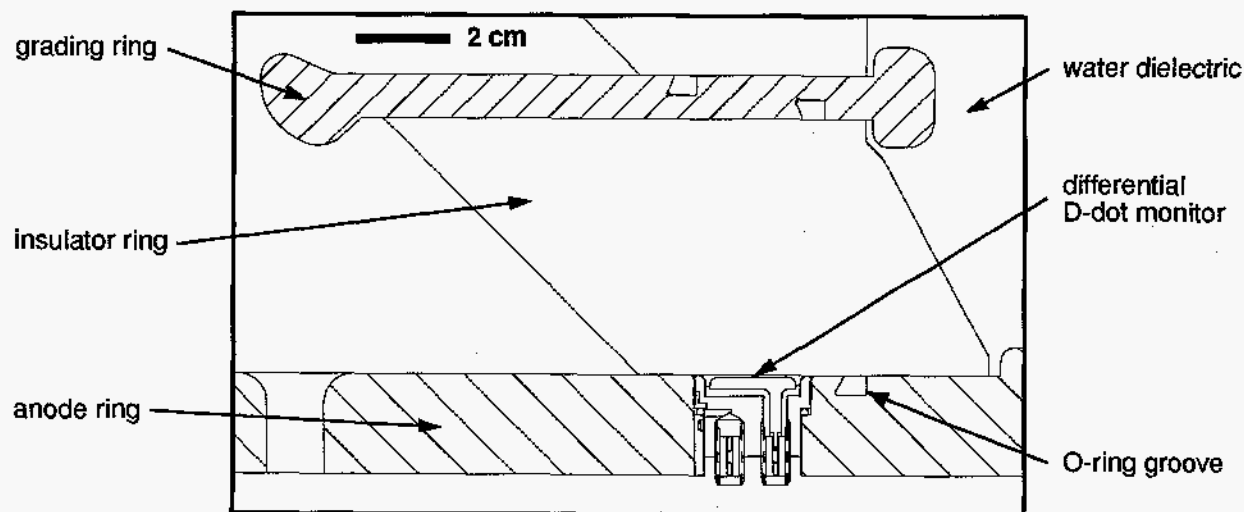


Figure 1. Detail of the Z insulator stack.

The design is detailed in Figure 2. One of the monitor's two outputs is connected to the displacement-current sensor; the other provides only a noise measurement. Two 2.2-mm-diameter Belden<sup>13</sup> RG-405 conformable coaxial cables connect the two outputs to a Prodyn<sup>14</sup> balun (model BIB-100B(mod)) for common-mode-noise rejection.<sup>15</sup> The cables provide reasonable bandwidth (power attenuation: 0.49 dB/m at 0.5 GHz) and generate acceptable levels of Compton drive.<sup>16</sup>

The D-dots are calibrated *in situ* with nine-module Z-accelerator shots that deliver power to a single MITL terminated with a short-circuit load. Faraday's law of induction is used to provide the reference voltage: the B-field is obtained from calibrated MITL B-dot monitors, and the geometry from the MITL and stack dimensions. A typical calibration result is presented in Figure 3. The nominal D-dot sensitivity is  $6.6 \times 10^{12}$  V/(m\*s\*V).

For a typical Z shot, the peak voltage at the balun output is 50-100 V during the main power pulse. Each of the 24 balun-output signals is reduced with a Weinschel<sup>18</sup> attenuator (model WA 1-20), recorded on a Tektronix<sup>19</sup> TDS-640 or TLS-216 0.5 ns/sample digitizing oscilloscope, and software cable compensated and integrated. The signals are recorded with long baselines to permit accurate baseline-offset calculations for the software integration.

### III. DIFFERENTIAL B-DOT DESIGN AND CALIBRATION

The differential B-dot design is outlined in Fig. 4. The 0.005-mm-thick nichrome film allows the B-field to penetrate but shields the epoxy and B-dot loops from the electric field. The two outputs have opposite polarities for common-

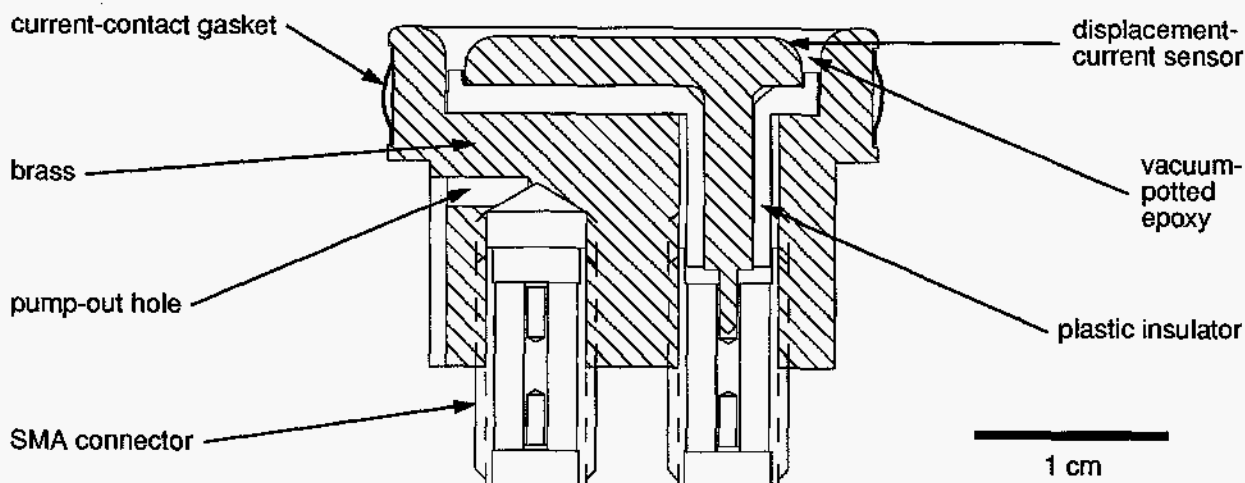
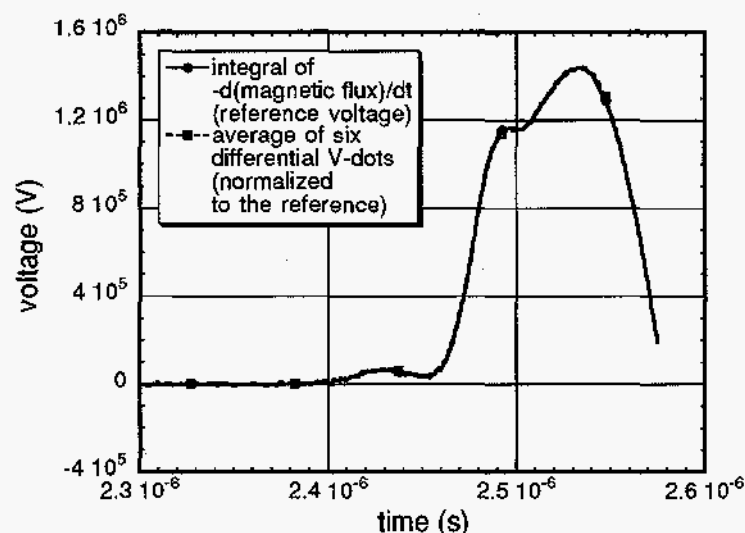


Figure 2. Detail of the differential D-dot monitor.



**Figure 3. Result of in situ calibration of the six differential D-dots in the D-level stack module. The normalized standard deviation of the difference in the two wave shapes<sup>17</sup> is less than 1%.**

mode-noise rejection. The output signals are processed as described for the differential D-dots (Sec. II).

The B-dots are calibrated with a 75-cm-diameter radial transmission line powered by a 5-kA pulse generator. The current wave shape of the system duplicates that of the Z accelerator. A precision 5-milliohm T&M Research<sup>20</sup> current-viewing resistor (model SSMA-2-005) mounted at the center of the transmission line measures the current. A typical calibration result is presented in Figure 5. The nominal B-dot sensitivity is determined to be  $1.5 \times 10^{11}$  A/(m\*s\*V). For a typical Z shot, the stack and MITL B-dot peak-output voltages (during the main power pulse) are approximately 50 and 100 V, respectively.

#### IV. CAVITY B-DOT DESIGN AND CALIBRATION

A new monitor is being developed to measure the total machine current 4.3 cm from the axis of the z-pinch load. The monitor, outlined in Fig. 6, measures the B-field that couples through a  $2.4 \times 4.8$  mm aperture into a 2.7-mm-tall 12.7-mm-diameter cavity. The design reduces the electron and z-pinch x-ray flux at the B-dot sensor and may prolong its lifetime in the high-energy-density environment. A differential measurement is obtained by fielding two monitors with opposite polarities at different azimuthal locations: the signals are recorded separately and common-mode-noise is subtracted in software. The signals (which peak at ~500 V) are reduced with Barth<sup>21</sup> (model 142-NMFP-26) attenuators before being recorded.

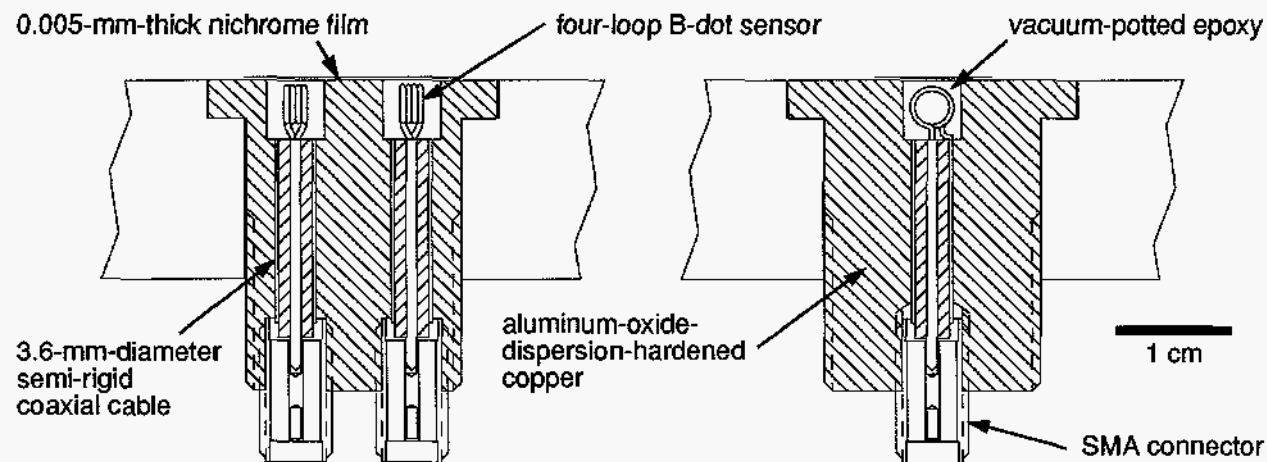


**Figure 4. Two views of the differential B-dot monitor.**

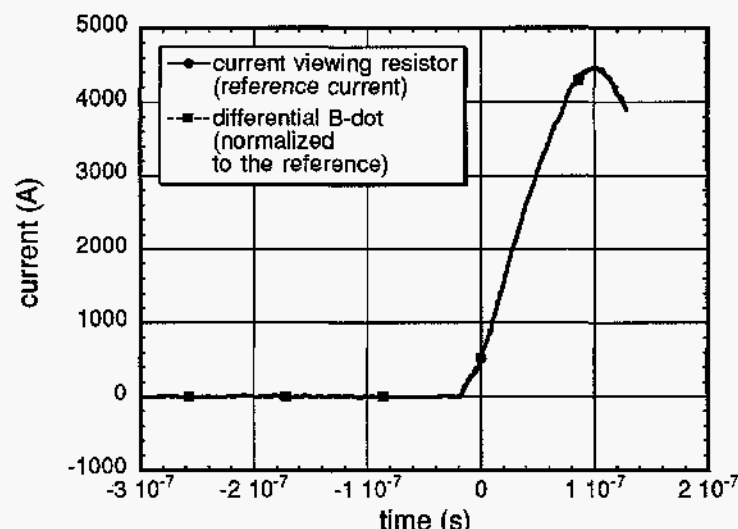


**Figure 5. Differential B-dot calibration result. The normalized standard deviation of the difference in the two wave shapes<sup>17</sup> is less than 1%.**

The monitor is calibrated with the same system used to calibrate the differential MITL and stack B-dots. Recent calibration results are presented in Figure 7. The B-dot sensitivity is typically  $1.6 \times 10^{12}$  A/(s\*V).

## V. Z-VACUUM-SECTION POWER-FLOW MEASUREMENTS

Measurements of the A-level stack voltage and MITL current (for Z-shot 66) are presented in Fig.'s 8 and 9. The effectiveness of the common-mode-noise rejection was determined with null measurements performed with monitors VSA260 and IMA300. Results, included in the Figures, indicate the residual noise can be neglected.

Measurements of the total Z current (for Z-shot 66) are presented in Fig. 10. The dip after peak current is due to the rapidly changing z-pinch inductance and is coincident with the emission of x-rays from the pinch. The principle limitation of this measurement appears to be closure of the aperture due to plasma formation by electron bombard-

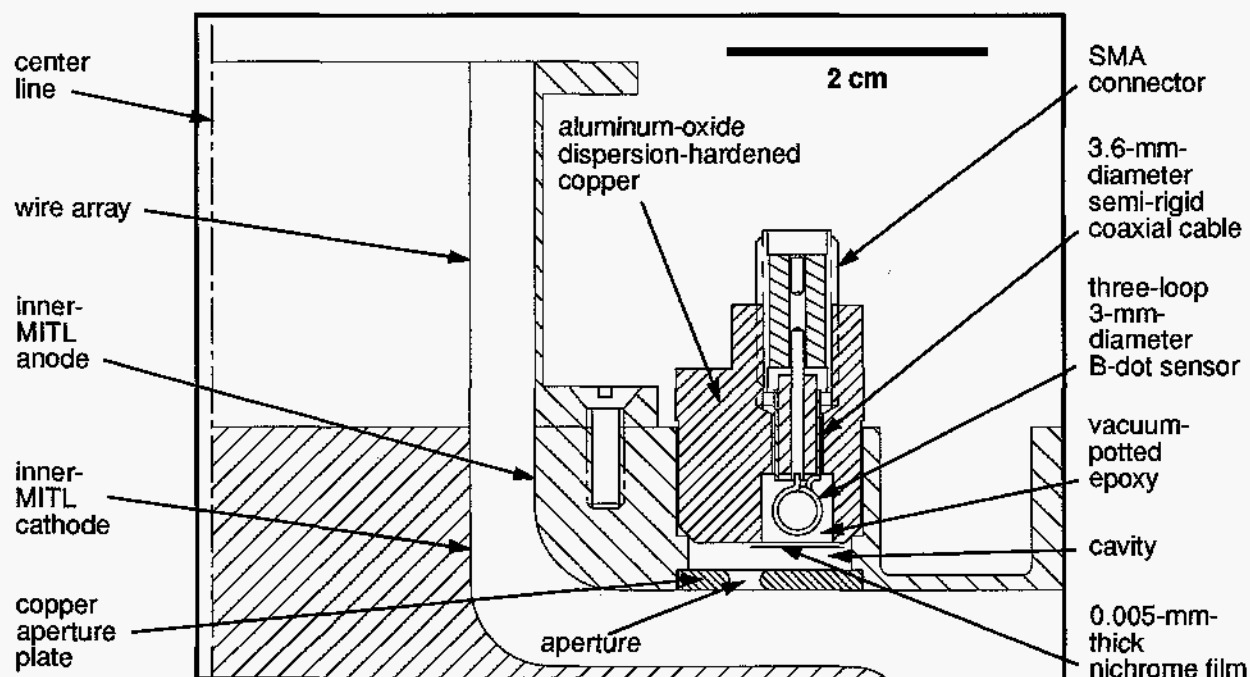


**Figure 6. Detail of the inner MITL and developmental cavity B-dot monitor.**

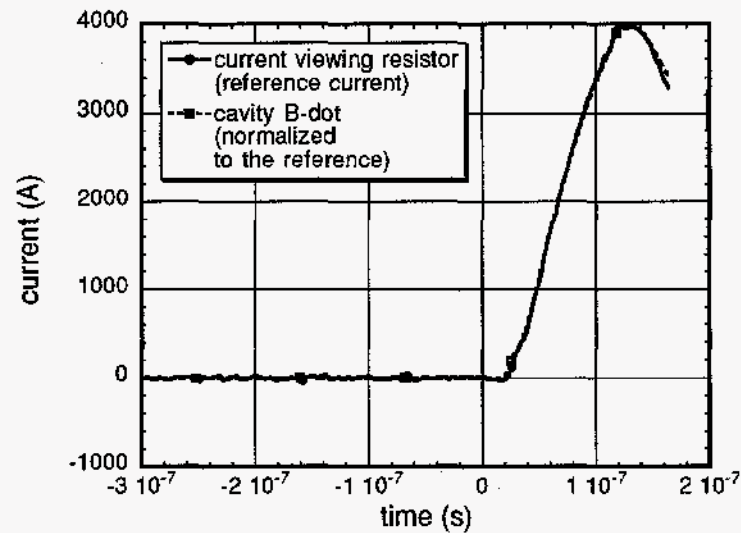


Figure 7. Cavity B-dot calibration result. The normalized standard deviation of the difference in the two wave shapes<sup>17</sup> is less than 1%.

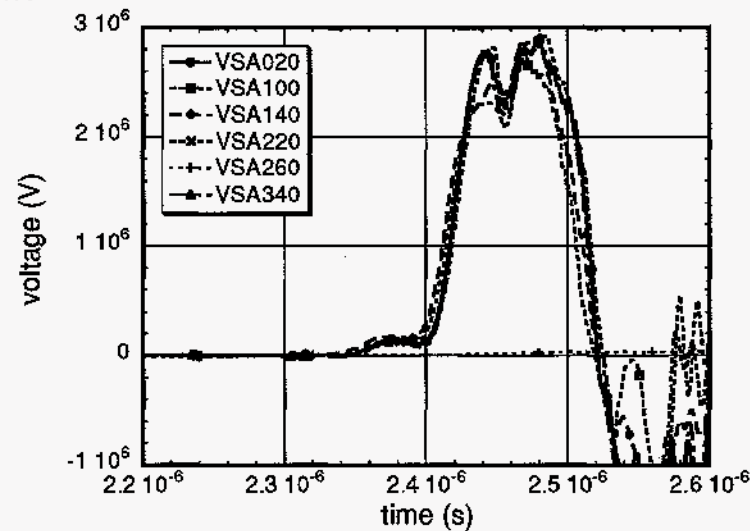


Figure 8. Measured A-level stack voltage at five azimuthal locations (Z-shot 66). Also plotted is a null measurement.

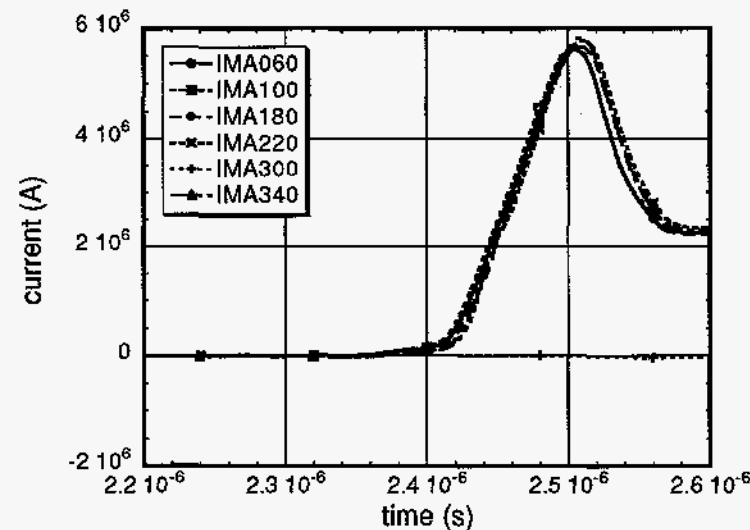


Figure 9. Measured A-level MITL current at five azimuthal locations (Z-shot 66). Also plotted is a null measurement.

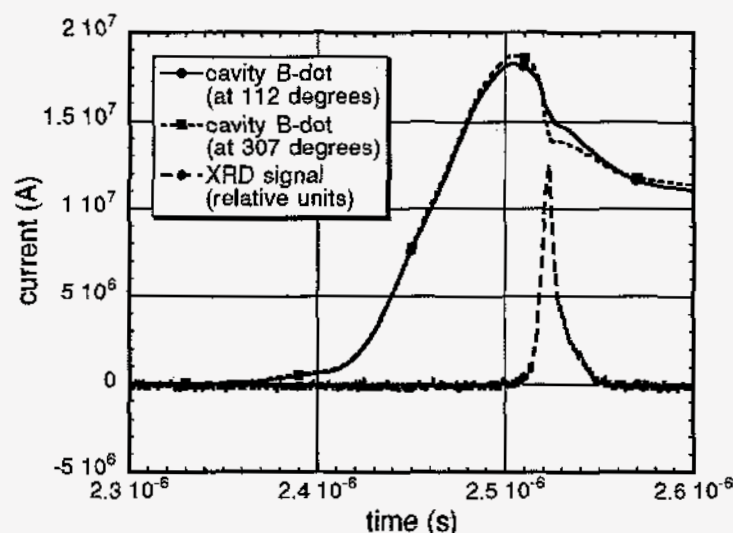


Figure 10. Measured total current 4.3 cm from the z-pinch load for Z-shot 66. The x-ray detector monitors radiation from the pinch.

ment and conduction-current heating.

#### ACKNOWLEDGEMENTS

The authors wish to thank W. Ballard, J. Barth, W. Beezhold, J. Boyes, R. Brockman, S. Downie, D. Droemer, D. Fehl, J. Gergel, J. Gergel, Jr., C. Guthrie, R. Hanes, D. Heath, K. Jones, J. Kellogg, M. Kernaghan, J. Lee, R. Leeper, F. Long, J. Martinez, M. Matzen, M. Mazarakis, D. McDaniel, J. McKenney, J. Melville, C. Mendel, Jr., G. Mowrer, T. Mullville, M. Pelock, D. Petnecky, B. Peyton, J. Powell, J. Ramirez, L. Reynolds, D. Rice, G. E. Rochau, T. Romero, R. Ross, J. H. Seamen, A. Seth, W. Simpson, I. Smith, J. Smith, S. Speas, R. Starbird, R. Valenzuela, R. Williams, L. Wilson, the Saturn and Z Operation Groups, Team Specialty Products, Bechtel Nevada, Prodyn Technologies, Barth Electronics, T&M Research Products, Votaw Precision Technologies, and Continental Machine Company for invaluable contributions. Sandia is a multiprogram laboratory operated by Sandia Corporation, a Lockheed Martin Company, for the United States Department of Energy under contract DE-ACO4-94AL85000.

<sup>1</sup>R. B. Spielman et. al., these proceedings.

<sup>2</sup>K. W. Struve, T. H. Martin et. al., these proceedings.

<sup>3</sup>R. J. Garcia et. al., these proceedings.

<sup>4</sup>W. A. Stygar, R. B. Spielman, G. O. Allshouse et. al., these proceedings.

<sup>5</sup>P. A. Corcoran et. al., these proceedings.

<sup>6</sup>H. C. Ives, D. M. Van De Valde et. al., these proceedings.

<sup>7</sup>Michael. A. Mostrom et. al., these proceedings.

<sup>8</sup>D. B. Seidel and C. W. Mendel, Jr., these proceedings.

<sup>9</sup>R. W. Shoup et. al., these proceedings.

<sup>10</sup>I. D. Smith et. al., these proceedings.

<sup>11</sup>K. W. Struve, M. L. Horry et. al., these proceedings.

<sup>12</sup>Integrated Engineering Software, Winnipeg, Manitoba, Canada

<sup>13</sup>Belden Wire and Cable Company, Richmond, Indiana, USA

<sup>14</sup>Prodyn Technologies, Albuquerque, New Mexico, USA

<sup>15</sup>G. E. Rochau, Sandia National Laboratories (private communication)

<sup>16</sup>W. P. Ballard and J. J. Hohlfelder, Sandia National Laboratories (private communication)

<sup>17</sup>L. P. Mix, Sandia National Laboratories (private communication)

<sup>18</sup>Weinschel, Bruno Associates, Gaithersburg, Maryland, USA

<sup>19</sup>Tektronix, Inc., Beaverton, Oregon, USA

<sup>20</sup>T&M Research Products, Inc., Albuquerque, New Mexico, USA

<sup>21</sup>Barth Electronics, Inc., Boulder City, Nevada, USA